

NEW RESEARCH PAPERS

Filamin C Truncation Mutations Are Associated With Arrhythmogenic Dilated Cardiomyopathy and Changes in the Cell-Cell Adhesion Structures



Rene L. Begay, MS,^a Sharon L. Graw, PhD,^a Gianfranco Sinagra, MD,^b Angeliki Asimaki, PhD,^c Teisha J. Rowland, PhD,^a Dobromir B. Slavov, PhD,^a Katherine Gowan, BS,^d Kenneth L. Jones, PhD,^d Francesca Brun, MD,^b Marco Merlo, MD,^b Daniela Miani, MD,^e Mary Sweet, BA,^a Kalpana Devaraj, MD,^f Eric P. Wartchow, BS,^g Marta Gigli, MD,^b Ilaria Puggia, MD,^b Ernesto E. Salcedo, MD,^a Deborah M. Garrity, PhD,^h Amrut V. Ambardekar, MD,^a Peter Buttrick, MD,^a T. Brett Reece, MD,ⁱ Michael R. Bristow, MD, PhD,^a Jeffrey E. Saffitz, MD, PhD,^c Luisa Mestroni, MD,^a Matthew R.G. Taylor, MD, PhD^a

ABSTRACT

OBJECTIVES The purpose of this study was to assess the phenotype of *Filamin C* (*FLNC*) truncating variants in dilated cardiomyopathy (DCM) and understand the mechanism leading to an arrhythmogenic phenotype.

BACKGROUND Mutations in *FLNC* are known to lead to skeletal myopathies, which may have an associated cardiac component. Recently, the clinical spectrum of *FLNC* mutations has been recognized to include a cardiac-restricted presentation in the absence of skeletal muscle involvement.

METHODS A population of 319 U.S. and European DCM cardiomyopathy families was evaluated using whole-exome and targeted next-generation sequencing. *FLNC* truncation probands were identified and evaluated by clinical examination, histology, transmission electron microscopy, and immunohistochemistry.

RESULTS A total of 13 individuals in 7 families (2.2%) were found to harbor 6 different *FLNC* truncation variants (2 stopgain, 1 frameshift, and 3 splicing). Of the 13 *FLNC* truncation carriers, 11 (85%) had either ventricular arrhythmias or sudden cardiac death, and 5 (38%) presented with evidence of right ventricular dilation. Pathology analysis of 2 explanted hearts from affected *FLNC* truncation carriers showed interstitial fibrosis in the right ventricle and epicardial fibrofatty infiltration in the left ventricle. Ultrastructural findings included occasional disarray of Z-discs within the sarcomere. Immunohistochemistry showed normal plakoglobin signal at cell-cell junctions, but decreased signals for desmoplakin and synapse-associated protein 97 in the myocardium and buccal mucosa.

CONCLUSIONS We found *FLNC* truncating variants, present in 2.2% of DCM families, to be associated with a cardiac-restricted arrhythmogenic DCM phenotype characterized by a high risk of life-threatening ventricular arrhythmias and a pathological cellular phenotype partially overlapping with arrhythmogenic right ventricular cardiomyopathy. (J Am Coll Cardiol EP 2018;4:504-14) © 2018 The Authors. Published by Elsevier on behalf of the American College of Cardiology Foundation. This is an open access article under the CC BY-NC-ND license (<http://creativecommons.org/licenses/by-nc-nd/4.0/>).

From the ^aCardiovascular Institute and Adult Medical Genetics Program, University of Colorado Denver, Aurora, Colorado; ^bDepartment of Cardiology, Ospedali Riuniti and University of Trieste, Trieste, Italy; ^cDepartment of Pathology, Beth Israel Deaconess Medical Center & Harvard Medical School, Boston, Massachusetts; ^dDepartment of Pediatrics, Section of Hematology, Oncology, and Bone Marrow Transplant, University of Colorado Denver, Aurora, Colorado; ^eDepartment of Cardiothoracic Science,

Dilated cardiomyopathy (DCM) is a major cause of heart failure and disproportionately leads to cardiac transplantation (1-3). The condition is familial in ~50% of cases, and genetic variants residing in over 40 genes have been found to cause DCM through a variety of pathological mechanisms associated with perturbations of the cytoskeleton, intercalated disc region, nuclear envelope, and muscle sarcomere (1,3). Filamin C (FLNC) is an actin cross-linking protein (4) that provides structure for the sarcomere and is one of the largest Z-disc proteins (2,725 amino acids) in cardiac and skeletal muscle. FLNC also localizes to the sarcolemma, where it connects the muscle cell to the extracellular matrix and is involved in related signaling pathways (5).

SEE PAGE 515

Originally, *FLNC* gene mutations were associated with distal and myofibrillar skeletal myopathies (MFM) (6), characterized by loss of myofibrils and filamentous intracellular aggregates of myocyte proteins, including desmin, dystrophin, and sarcoglycans. Further investigations have revealed that *FLNC* missense mutations may lead to hypertrophic cardiomyopathy (HCM) (7) and restrictive cardiomyopathy (RCM) (8). Recently, using whole exome sequencing, we identified an *FLNC* splicing variant as causing DCM in the absence of skeletal muscle involvement in 2 families (9), a finding further supported by the report of *FLNC* truncation variants in 4% of DCM and 3% of arrhythmogenic DCM patients (10-12).

In the current study, we report the characterization of the clinical features of *FLNC* truncating variant carriers, which include a prominent arrhythmogenic DCM phenotype (13), sarcomere structural changes by transmission electron microscopy (TEM), and changes in the distribution of cell-cell junction proteins in the myocardium and buccal mucosa. These structural and cellular changes overlap with arrhythmogenic right

ventricular cardiomyopathy (ARVC), and represent a critical link between DCM and ARVC, leading to a more comprehensive understanding of complex familial arrhythmia syndromes as well as an appreciation of the need for mutation-directed clinical monitoring and treatment of this population.

METHODS

STUDY POPULATION AND CARDIOMYOPATHY EVALUATION. We analyzed 319 U.S. and European DCM families from the Familial Cardiomyopathy Registry. Study subjects underwent extensive clinical evaluations (details in the [Online Appendix](#)) (14). Medical records from deceased subjects were reviewed when available (9). Informed consent was obtained from living subjects, and local institutional review boards approved the study protocols.

NEXT-GENERATION SEQUENCING AND BIOINFORMATIC ANALYSIS. Twenty larger families were evaluated by whole-exome sequencing (9). In 299 smaller families, probands were evaluated using the Illumina TruSight One-Sequence panel (Illumina, Redwood City, California), which queries 4,813 genes associated with known clinical phenotypes (15). Briefly, subject deoxyribonucleic acid (DNA) was captured with the panel, sequenced on an HISEQ 2500 (Illumina) with v4 chemistry, and mapped with Genomic Short-read Nucleotide Alignment Program (version 2012-07-20) (16). Variants were called with the Genome Analysis Toolkit (version 2.1-8-g5efb575, Broad Institute, Cambridge, Massachusetts) and classified with Annovar (version 2012-07-28) (17). Functional predictions were made with the database for Nonsynonymous SNPs and Their Functional Predictions (version 2.0) (18). All variants were confirmed by Sanger sequencing (19). Variants

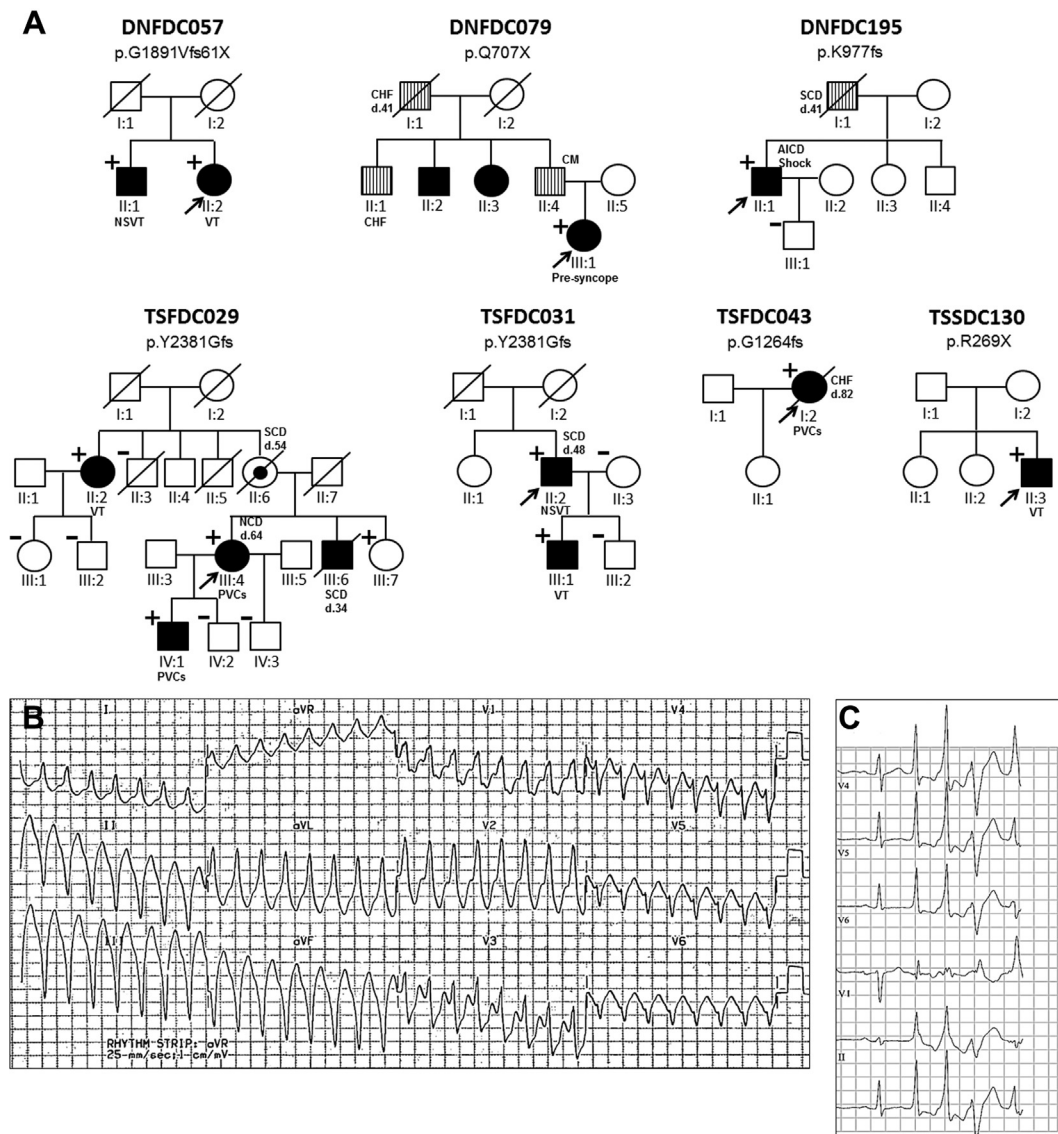
ABBREVIATIONS AND ACRONYMS

Cx43	= connexin 43
DCM	= dilated cardiomyopathy
DNA	= deoxyribonucleic acid
ExAC	= Exome Aggregation Consortium
FLNC	= Filamin C
SK3β	= glycogen synthase kinase 3 beta
HCM	= hypertrophic cardiomyopathy
LV	= left ventricle/ventricular
MFM	= myofibrillar skeletal myopathy
RNA	= ribonucleic acid
RV	= right ventricle/ventricular
SAP97	= synapse-associated protein 97
SCD	= sudden cardiac death
TEM	= transmission electron microscopy

University Hospital S. Maria della Misericordia, Udine, Italy; ^fDepartment of Pathology, University of Colorado, University Hospital, Aurora, Colorado; ^gDepartment of Pathology, Children's Hospital Colorado, Aurora, Colorado; ^hCenter for Cardiovascular Research and Department of Biology, Colorado State University, Fort Collins, Colorado; and the ⁱDepartment of Surgery, University of Colorado Denver, Aurora, Colorado. This study was supported by National Institutes of Health grants R01 HL69071 and HL116906 (to Dr. Mestroni), R01 116906 (to Dr. Saffitz), and 1K23HI067915 and R01HL109209 (to Dr. Taylor); and by the CRTrieste Foundation and GENERALI Foundation (to Dr. Sinagra). This work is also supported in part by a Trans-Atlantic Network of Excellence grant from the Leducq Foundation (14-CVD 03) and by National Center for Advancing Translation Sciences at the National Institutes of Health Colorado CTSA Grant Number UL1 TR001082. Dr. Mestroni has served as a consultant for Array BioPharma. Dr. Taylor has served on the Speakers Bureau of GeneDx. All other authors have reported that they have no relationships relevant to the contents of this paper to disclose.

All authors attest they are in compliance with human studies committees and animal welfare regulations of the authors' institutions and Food and Drug Administration guidelines, including patient consent where appropriate. For more information, visit the [JACC: Clinical Electrophysiology author instructions page](#).

Manuscript received October 5, 2017; revised manuscript received November 20, 2017, accepted December 7, 2017.

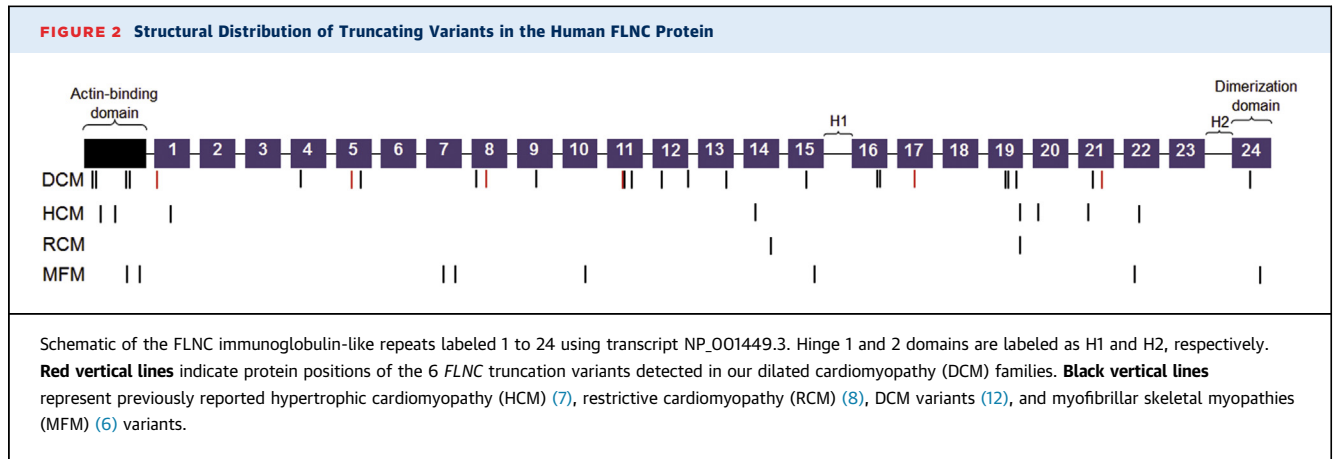
FIGURE 1 Pedigrees of DCM Families With *FLNC* Truncating Variants Displaying an Arrhythmogenic Phenotype

(A) Squares indicate males, circles indicate females, slashes indicate deceased individuals, black shading indicates a dilated cardiomyopathy (DCM) phenotype, and vertical lines indicate history of heart disease. The arrows indicate the proband. Carriers (+) and noncarriers (–) of a *FLNC* truncation variant are shown. **(B)** Electrocardiogram of subject TSSDC130 (II:3) shows sustained ventricular tachycardia. **(C)** Electrocardiogram depicts nonsustained ventricular tachycardia from individual II:1 (family DNFD057) (9).

predicted to be damaging in at least 1 of the prediction algorithms were retained, whereas missense and truncation variants present in >1% in the 1000 Genomes Project were discarded (9,20).

Variant frequency information was obtained from the 6,500 National Human, Lung, and Blood Institute Exome Sequencing Project (21) and the Exome Aggregation Consortium (ExAC, Cambridge, Massachusetts) (22) on February 27, 2017, and was

cross-referenced to the ClinVar database (23). Gene variant locations are provided in reference to *FLNC* transcript NM_001458. Cosegregation analysis was performed when DNA from biological relatives was available. Variants in other cardiomyopathy-related genes were also identified using the Illumina TruSight One Sequencing Panel, as described in the previous text, and confirmed using Sanger sequencing.



HISTOLOGY AND TRANSMISSION ELECTRON MICROSCOPY. Cardiac muscle tissue was obtained from 2 affected siblings of family DNFDC057 (Figure 1), including left ventricular (LV) tissue at the time of LV assist device placement in subject II:1 and LV and right ventricular (RV) tissue from the explanted heart of subject II:2. Fresh heart tissue samples were processed according to standard histology protocols for hematoxylin and eosin, Masson’s trichrome, and immunohistochemistry staining and fixed for TEM. Details can be found in the Online Appendix.

IMMUNOSTAINING. Cotton-tipped swabs (Medi-Choice, Mechanicsville, Virginia) were used to collect buccal mucosa cells from 2 siblings with truncating variants in *FLNC* and from normal control subjects. Each cheek was rubbed with a slight rolling and scraping motion, and the resulting material was smeared on standard microscope slides. Immunostaining of buccal mucosa and myocardial tissue was performed as previously described (24), and is detailed in the Online Appendix. For immunofluorescence microscopy, antibodies included: mouse monoclonal antiplakoglobin (P8087, Sigma-Aldrich, St. Louis, Missouri), mouse monoclonal anti-connexin 43 (Cx43) (Millipore, Burlington, Massachusetts), mouse monoclonal anti-N-cadherin (Sigma-Aldrich), mouse monoclonal antidesmoplakin (Fitzgerald, Acton, Massachusetts), mouse monoclonal anti-synapse-associated protein 97SAP97 (Santa Cruz, Dallas, Texas), and rabbit polyclonal antiglycogen synthase kinase 3 β (GSK3 β) (Cell Signaling Technology, Danvers, Massachusetts). Immunostained preparations were analyzed by confocal microscopy (LSM-510, Zeiss, Oberkochen, Germany).

RIBONUCLEIC ACID SEQUENCING OF EXPLANTED HEART TISSUE. Ribonucleic acid (RNA) was extracted from frozen LV tissue using the mirVana miRNA

isolation kit (Thermo Fisher Scientific, Waltham, Massachusetts) enriched for total RNA according to manufacturer’s instructions with the exception of replacing the lysis/binding buffer with mechanical homogenization in TRIzol (Thermo Fisher Scientific). The library was sequenced 1 \times 50 (Illumina HiSeq 2500). Reads were filtered for quality and aligned to the GRCh37hg19 reference human genome using the Genomic Short-read Nucleotide Alignment Program. Transcripts aligning to *FLNC* were visualized using the Integrative Genomics Viewer (Broad Institute).

RESULTS

IDENTIFICATION OF *FLNC* TRUNCATIONS. Pathogenic/likely pathogenic variants have been identified in approximately 40% of dilated cardiomyopathy samples from the Familial Cardiomyopathy Registry (data not shown), and include *TTN* (11%), sarcomeric genes (10%), structural cytoskeleton genes (5%), *LMNA* (4%), ion channel genes (2%), and other rare genes (5%). A total of 6 *FLNC* truncation variants (Figure 1), including 2 *FLNC* stopgain (families DNFDC079 and TSSDC130), 1 frameshift (DNFDC057), and 3 splicing variants (families DNFDC195, TSFDC029, TSFDC031, and TSFDC043), were identified in 7 of the 319 DCM families, for an overall frequency of 2.2% (7 of 319) (Figure 2, Table 1), 100-fold more frequent than the 0.02% *FLNC* loss of function variants reported in ExAC (22). Five of the *FLNC* truncation variants were absent from the 1000 Genomes Project, 6,500 Exome Sequencing Project, ExAC, and ClinVar databases; c.805C>T had a minor allele frequency of 8.3×10^{-6} in ExAC (Online Table 1). *FLNC* variants p.Y2381Gfs21X and p.G1891Vfs61X have been previously reported (9). The 6 *FLNC* truncation variants reported here (Figures 1 and 2) occur in the immunoglobulin domains of the

TABLE 1 Clinical Phenotype Features of FLNC Truncation Carriers and DCM-Affected Individuals

Family	DNFDC057		DNFDC079	DNFDC195	TSFDC029	
Individual	II:1	II:2	III:1	II:2	II:2	III:4
Sex	M	F	F	M	F	F
Age at diagnosis, yrs	59	54	33	39	62	46
Variation	Frameshift		Stopgain	Splicing	Splicing	
Nucleotide change	c.5669-1delG		c.2119C>T	c.2930-1G>T	c.7251+1A>G	
AA change	p.G1891Vfs61X		p.Q707X	p.K977fs	p.Y2381Gfs	
Secondary mutation						
NYHA functional class	III	II	III	II	I	II
Symptoms	DOE, fatigue	Palpitations, SOB	Pre-syncope, SOB	Syncope	Palpitations	Palpitations, SOB, chest pain
Arrhythmias	PACs, PVCs, NSVT	PVCs, AF, sustained VT (1997)	No arrhythmias	Multiform PVCs	Sustained VT, PVCs (800/24 h), NSVT	PVCs (900/24h), NSVT
ECG	AVB1, incomplete LBBB	AVB1, LVH	Nonspecific ST changes	PM, AICD, nonspecific ST changes	PVCs	Low voltages
LVEDD, cm	6.4	5.6	5.4	7.2	5.4, inferobasal hypokinesia	5.5
LVEF, %	45	10	20	15	52	32
CK, U/l†	118	106	56	NA	56	32
RV	Normal	Mild dilatation	Dilatation	Mild dilatation and dysfunction	Normal (FS 53%)	Normal (FS 60%)
Outcome	NYHA functional class II, LVEF 21%, CRT, AICD, LVAD (2016)	Severe LV and RV dysfunction, heart transplant (2009)	Normalized LVEF 60%	Appropriate AICD discharge (2016)	NYHA functional class I, LVEF 51%	NYHA functional class II, NCD
Follow-up, yrs	11	11	1	6	15	14

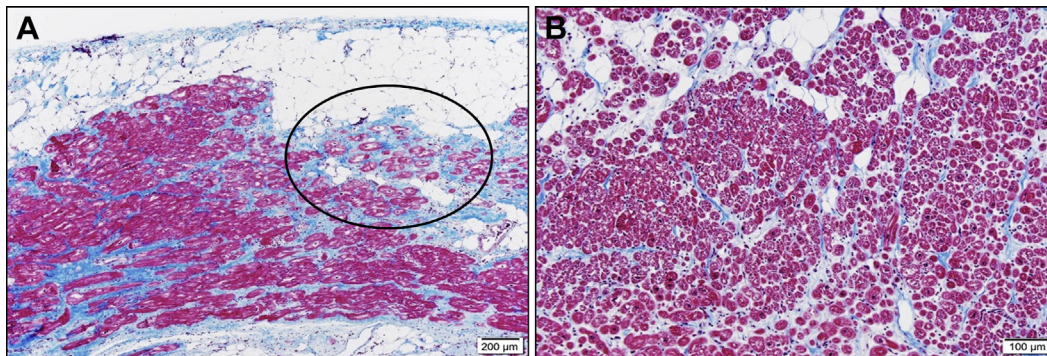
TABLE 1 Continued

Family	TSFDC029		TSFDC031	TSFDC043	TSSDC130	
Individual	III:6*	III:7	IV:1	II:2	III:1	II:3
Sex	M	F	M	M	M	F
Age at diagnosis, yrs	35	34	27	44	20	76
Variation	Splicing		Splicing	Splicing	Splicing	Stopgain
Nucleotide change	c.7251+1A>G		c.7251+1A>G	c.3791-1G>A	c.805C>T	
AA change	p.Y2381Gfs		p.Y2381Gfs	p.G1264fs	p.R269X	
Secondary mutation						
SCN5A c.5270delT; p.F1757fs						
NYHA functional class	I	I	II	II	I	II
Symptoms	Asymptomatic, SCD	Palpitations	Fatigue, palpitations	SOB	Pre-syncope	Fatigue, SOB
Arrhythmias	NA	No arrhythmias	PACs, PVCs (93/24h)	NSVT, couplet (154/24h)	PAF, SVT, SAECG	AF, frequent PVCs
ECG	NA	Normal	RBBB	Normal	Normal	AVB, RBBB, LAFB
LVEDD, cm	NA	4.9	5.3	5.7	5.5, inferobasal hypokinesia	6.4
LVEF, %	NA	63	45	47	45	14
CK, U/l†	NA	50	80	103	70	NA
RV	NA	Normal	Normal	NA	Mild dilatation and dysfunction (FS 33%)	Dilatation and dysfunction
Outcome	Cardiomegaly at autopsy	NYHA functional class I	NYHA functional class I, palpitations, LVEF 52%	NYHA functional class II, SCD	NYHA functional class I, palpitations, LVEF 40%	PM, heart failure death (2008)
Follow-up, yrs		15	15	4	17	9
						Recurrent sustained VT, AICD (1999), NYHA functional class II
						14

Families DNFDC057, TSFDC029, and TSFDC031 are previously reported variants (9). *Individual III:6 died before enrollment; DNA was not available for genetic testing. †Normal CK level is <223 U/L.

AA = amino acid; AF = atrial fibrillation; AICD = automatic implantable cardioverter-defibrillator; AVB = atrioventricular block; CK = creatine kinase; CRT = cardiac resynchronization therapy; DOE = dyspnea on exertion; ECG = electrocardiogram; FS = fractional shortening; IV = intraventricular; LAFB = left anterior fascicular block; LBBB = left bundle branch block; LVAD = left ventricular assist device; LVEDD = left ventricular end-diastolic dimension; LVEF = left ventricular ejection fraction; LVH = left ventricular hypertrophy; NA = not available; NCD = noncardiac death; NYHA = New York Association functional class; PAF = paroxysmal atrial fibrillation; PM = pacemaker; PAC = premature atrial contraction; PVC = premature ventricular contraction; RBBB = right bundle branch block; RV = right ventricle; SAECG = signal-averaged electrocardiography; SB = sinus bradycardia; SCD = sudden cardiac death; SOB = shortness of breath; ST = sinus tachycardia; VT = ventricular tachycardia.

FIGURE 3 Cardiac Tissue Analysis of *FLNC* Truncation Variant Carrier From Family DNFDC057 (II:2)



(A) Trichrome staining of the left ventricle shows subepicardial interstitial and focal replacement fibrosis and fatty infiltration (**circle**) in areas containing degenerating cardiac myocytes. Scale bar = 200 μ m. **(B)** Fatty infiltration and mild fibrosis are seen in the right ventricle. Scale bar = 100 μ m.

FLNC protein with no apparent geographical clustering or relationships to HCM, RCM, and MFM *FLNC* variants described to date. The presence of a secondary “likely pathogenic” unique variant was found in a known cardiomyopathy-related gene in the TSFDC043 proband (*SCN5A* c.5270delT; p.F1757fs, not reported in ExAC and ClinVar databases) who did not show signs of Brugada or long QT syndromes. Finally, *FLNC* missense variants detected in the overall population of 319 families are charted to the *FLNC* protein in [Online Figure 1](#) and details are reported in [Online Table 2](#).

RNA-Seq was performed on the explanted heart of DNFDC057 patient II:2. The majority of *FLNC* transcripts (141 of 162 total reads; 87.0%) were wildtype, and the remaining reads predominantly contained the c.5669-1delG, resulting in a frameshift and subsequent premature stop codon (as nucleotide 5670 is also a G, splicing occurs normally but introduces a frameshift into exon 34). These data support a mechanism of nonsense-mediated decay leading to haploinsufficiency, consistent with our zebrafish studies in which morpholino knockdown of the *flnbc* transcript led to a cardiac phenotype.

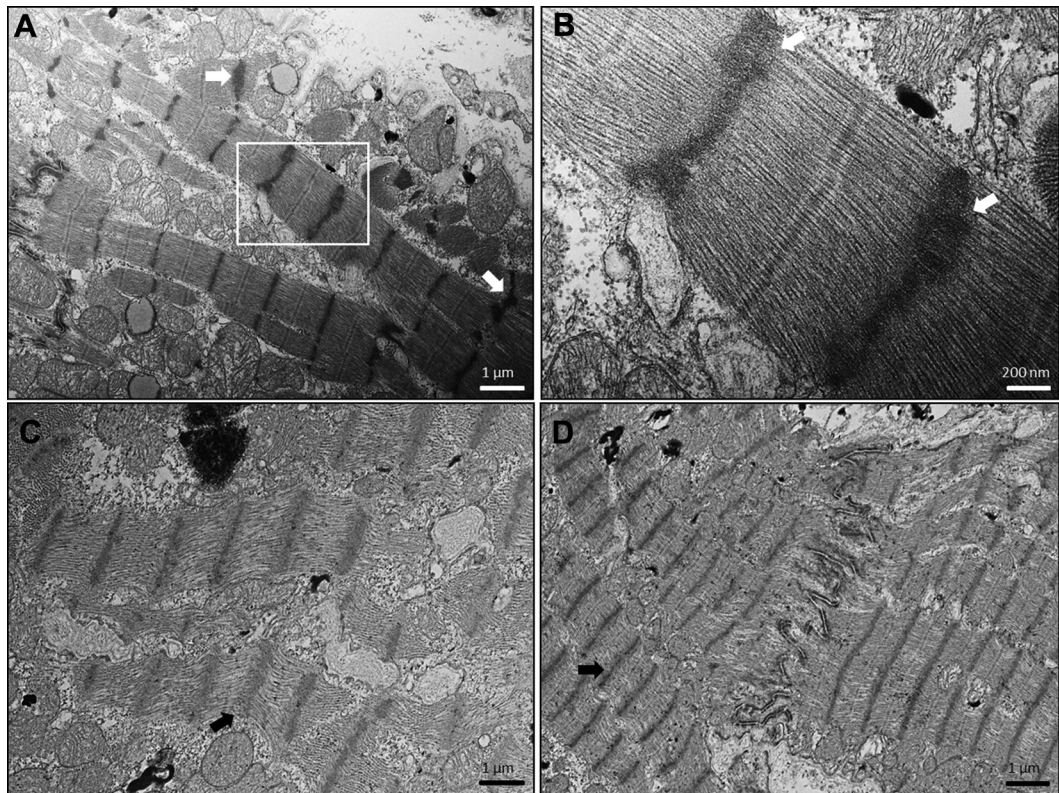
CLINICAL PHENOTYPES OF *FLNC* TRUNCATION AFFECTED INDIVIDUALS. Clinical features of *FLNC* truncation carriers are reported in [Table 1](#), and a detailed clinical description is reported in the [Online Appendix](#). None of the patients fulfilled Task Force criteria of ARVC (25). Comprehensive physical examination of the skeletal muscle of all probands revealed no skeletal muscle abnormalities; serum creatine kinase levels were normal in all tested probands.

Supraventricular and ventricular arrhythmias as well as conduction disease were prominent clinical features ([Figure 1](#), [Table 1](#)). Ventricular arrhythmias appear to originate from the LV or appeared polymorphic. Sudden cardiac death (SCD) occurred before the age of 55 years in 5 of 22 (23%) confirmed ($n = 13$) or suspected by family history ($n = 9$) truncation carriers. RV involvement with dilatation and/or dysfunction was present in 5 of 13 (38%) cases. The overall penetrance of *FLNC* truncation variants in our 7 families was 92% (1 unaffected of 13 total confirmed truncation carriers).

HISTOLOGICAL AND ULTRASTRUCTURAL CARDIAC ANALYSIS OF *FLNC* G1891Vfs61X VARIANT.

Cardiac muscle tissue was studied from 2 affected siblings of family DNFDC057. In the proband II:2, light microscopic analysis of the LV from the explanted heart showed myocyte hypertrophy, diffuse interstitial fibrosis, and focal replacement fibrosis ([Figure 3A](#)). Epicardial fat tissue infiltrated focally into the LV myocardium, especially in areas of replacement fibrosis containing clusters of degenerating myocytes with myofibrillar loss ([Figure 3A](#)). The RV showed increased interstitial fibrosis and mild fatty infiltration ([Figure 3B](#)). In the affected sibling II:1, cardiac tissue taken upon LV assist device placement showed similar cardiac tissue pathology in the LV ([Online Figure 2](#)).

Ultrastructural analysis of LV tissue of affected patient II:1 (DNFDC057) using TEM ([Figures 4A and 4B](#)) revealed largely normal sarcomere structures, although abnormal Z-discs were noted. In LV tissue from individual II:2 and II:1 (DNFDC057), the Z-discs appeared less compact and diffuse along the

FIGURE 4 Electron Microscopy Images of Left Ventricular Cardiac Muscle From Family DNFD057

(A) Representative images from individual II:2 show disarrayed Z-discs (white arrows). (B) Magnified image of the white box in A, showing a thickened Z-disc pattern. (C and D) Representative TEM images from individual II:1 exhibiting disarray of Z-discs (black arrows). No aggregates are seen in cardiac myocytes. Scale bars: (A) 1 μ m, (B) 200 nm, (C and D) 1 μ m.

Z-disc axis (Figures 4C and 4D). In contrast to MFM cases, no intracellular aggregates were seen.

IMMUNOHISTOCHEMICAL ANALYSIS OF FLNC AND ARRHYTHMOGENIC-ASSOCIATED PROTEINS.

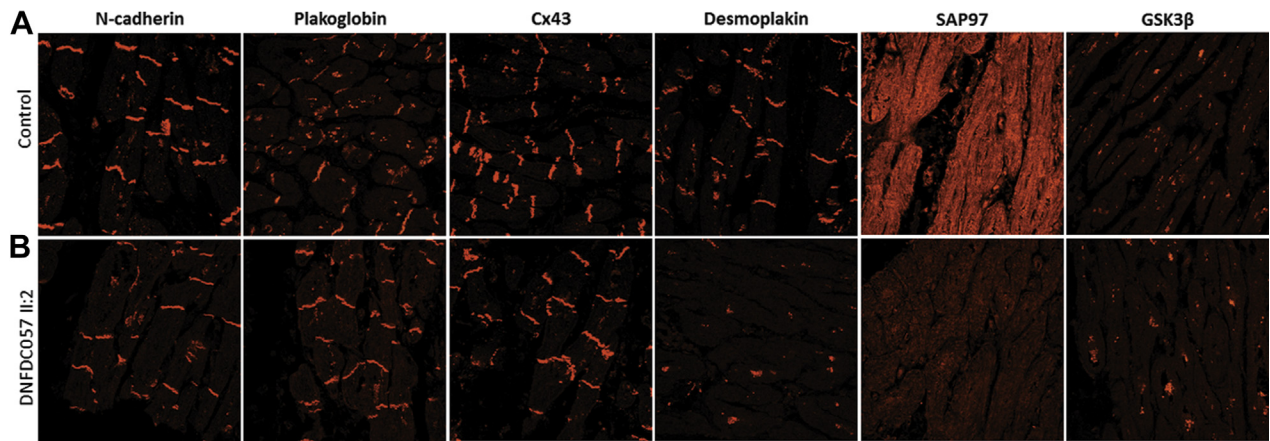
Abnormalities in the distribution and expression of desmosomal and gap junction proteins have been reported in cardiac tissue of patients with arrhythmogenic cardiomyopathy (26). Because some of the clinical (SCD, ventricular arrhythmia) and structural (RV involvement, fibrofatty infiltration) features in our FLNC patients mirrored features of arrhythmogenic cardiomyopathy, we used immunohistochemistry to characterize selected protein distribution in the LV myocardial tissue in affected individual II:2 of family DNFD057 (Figure 5).

Immunohistochemistry staining for the desmosomal protein desmoplakin and SAP97, a membrane-associated guanylate kinase involved in trafficking sodium and potassium channel subunits to the cell surface, revealed overall decreased signal intensity

for both of these proteins compared with healthy control tissues (Figure 5), agreeing with previous studies that showed decreased expression of these proteins in ARVC (27). Additionally, staining for GSK3 β revealed that this protein retained its cytoplasmic distribution and did not translocate to the intercalated discs, which has been shown previously to occur in classical ARVC (28). Last, staining for the desmosomal protein plakoglobin and the major cardiac gap junction protein Cx43 (normally located in the intercalated discs) revealed these proteins to have immunoreactive signals similar in intensity and distribution to the healthy control tissues, although the expression of these proteins is usually reduced at cardiac cell-cell junctions in classical ARVC (26,27). Immunohistochemical staining of FLNC revealed no significant intracellular protein aggregates in cardiac myocytes (Figure 6).

Desmosomal and gap junction protein abnormalities have similarly been previously reported in the

FIGURE 5 Immunohistochemistry of Left Ventricular Myocardial Tissue



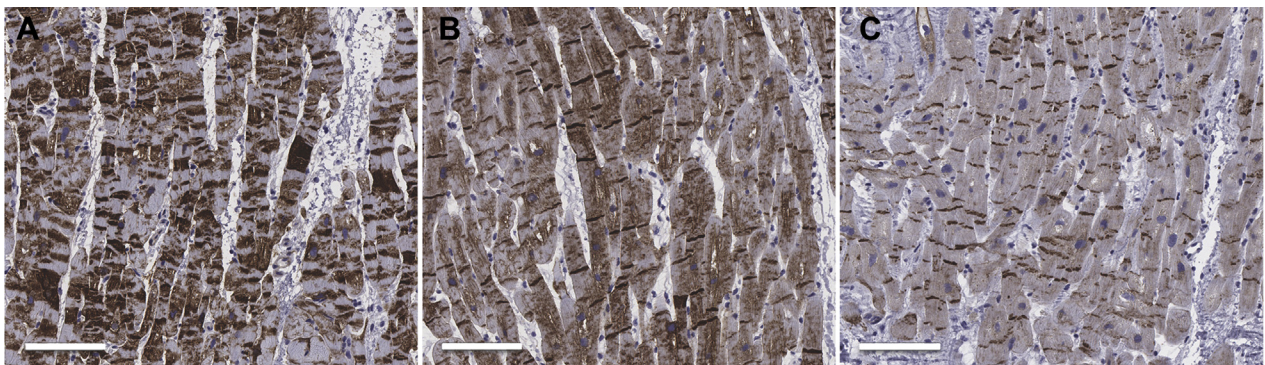
Immunostaining of the explanted heart of patient DNFDC057-II:2 carrying the G1891Vfs61X *FLNC* truncation. (A) Immunoreactive signals for plakoglobin and connexin 43 (Cx43) at intercalated discs are normal compared with control samples, whereas junctional signal for desmoplakin is reduced. N-cadherin is used as a tissue quality control and is normal in all samples. (B) SAP97 signal is depressed compared with control samples. GSK3β maintained its normal cytoplasmic distribution.

buccal mucosa of patients with ARVC (26), which led us to also perform immunostaining of buccal mucosa smears obtained from affected patients DNFDC057 II:1 and II:2 (Figure 7). Our buccal mucosa cell staining results were generally concordant with the LV myocardial immunostaining of patient II:2, including diminished signal intensity for desmoplakin and SAP97, and signal intensity near normal levels for plakoglobin. However, unlike the normal levels of Cx43 observed in the LV myocardial immunostaining, staining for Cx43 was found to be reduced in the buccal mucosa cells.

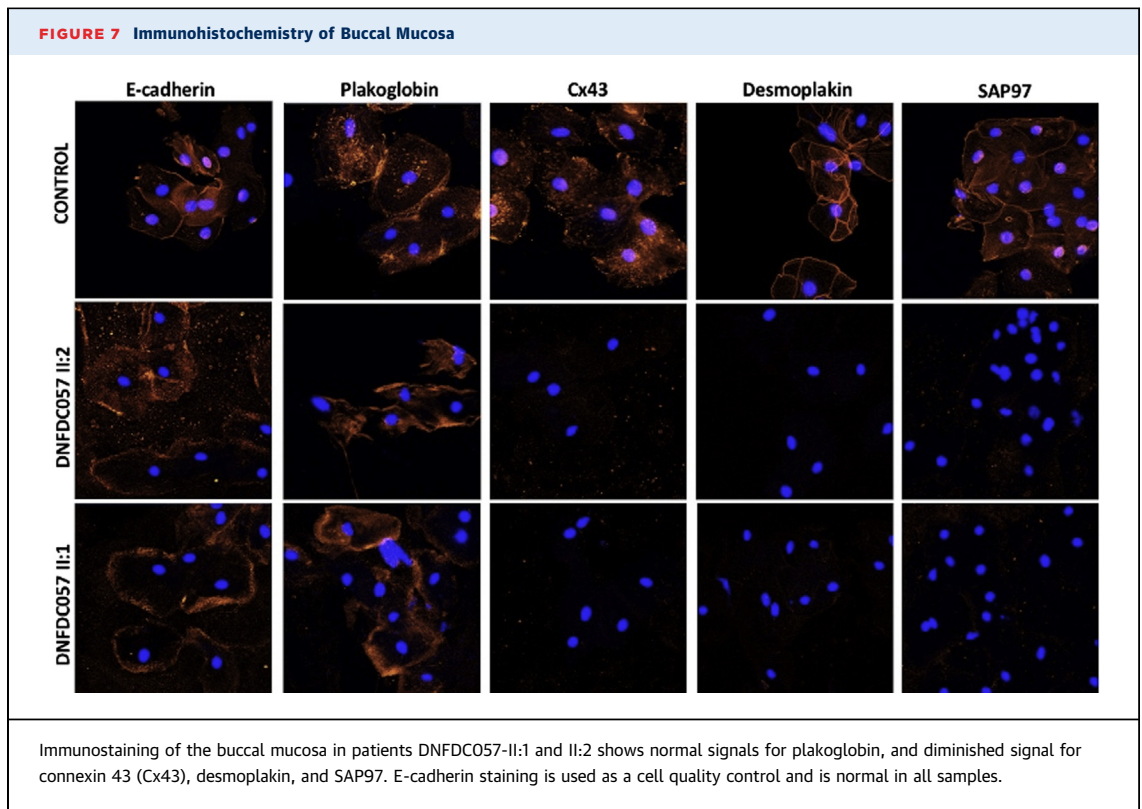
DISCUSSION

In a cohort of 319 DCM families, prospectively enrolled in the Familial Cardiomyopathy Research Registry at the University of Colorado Hospital and Azienda Sanitaria Universitaria Integrata of Trieste Hospital, we identified 7 families (2.2%) harboring 6 different *FLNC* truncation variants distributed across the *FLNC* gene. These truncation carriers had a prominent arrhythmogenic phenotype characteristic of arrhythmogenic DCM, family history of SCD, frequent RV involvement, and displayed no clinical signs of

FIGURE 6 FLNC in Cardiac Tissue



Immunohistochemical staining of FLNC does not show significant presence of aggregates in cardiomyocytes, and the weaker staining in the patient (C) suggests a reduced amount of FLNC protein compared with control subjects (A and B), as previously shown by western blot (9).



skeletal muscle involvement. As we previously reported, arrhythmogenic DCM patients have a higher risk for life-threatening ventricular arrhythmias and SCD, in particular when a family history of SCD is present, highlighting the importance of early identification of patients carrying *FLNC* truncation variants (13).

Filamins are large cytoskeletal actin cross-linking proteins that stabilize the actin filament networks and link them to the cell membrane by binding transmembrane proteins and ion channels (29). *FLNC* encodes a large protein (2,725 amino acids) primarily expressed in the cardiac and skeletal muscle that interacts with sarcomeric proteins in the Z-disc and the sarcolemma (6). Mutations in *FLNC* were initially reported to cause MFM (6), while cardiac involvement may have been noted, but not studied extensively. A study of German families with the p.Trp2710* founder mutation reported that 8 of 31 patients had LV hypertrophy, atrial flutter, and right bundle branch block (30). More recent reports support *FLNC* involvement in a spectrum of cardiomyopathies, including HCM, RCM, and DCM, where arrhythmias, cardiac conduction disease, and SCD were also described (7,8) in the absence of skeletal muscle pathology (7-12). Similarly, our *FLNC* truncation carriers also exhibited no clinical evidence of skeletal muscle abnormalities. Our current report

provides additional evidence of an arrhythmogenic DCM phenotype likely caused by *FLNC* truncation variants, including LV dysfunction, RV involvement, severe arrhythmias, and conduction disease.

All variants identified in our study are expected to lead to a truncated or absent *FLNC* protein. Our analysis of *FLNC* transcripts revealed that most (87.0%) were wildtype, suggestive of a haploinsufficiency model. This agrees with our previous investigation reporting that explanted heart tissue from a *FLNC* truncation carrier had reduced levels of *FLNC* protein compared with healthy control samples by Western blot, lending support for a haploinsufficiency mechanism of *FLNC* pathology (9). We also previously found that a reduction in *flncb* (ortholog of human *FLNC*) RNA expression in zebrafish results in structural and functional cardiac abnormalities (9), further supporting the theory that reduced *FLNC* expression may result in the observed cardiac dysfunctions.

We additionally found irregular and thickened Z-discs in the tissue of *FLNC* truncation carriers (Figures 4A to 4D). Similarly, in our *flncb* MO knock-down zebrafish model, the cardiac muscle ultrastructure displayed prominent Z-disc disarray and malformations, and in some instances the Z-disc was absent (9). Surprisingly, our current study did not find cytoplasmic protein aggregates in the heart, which

have been described previously in *FLNC*-associated patients with MFM (in muscle biopsies) as well as HCM and RCM patients (7,8). In these cases, accumulations of protein aggregates are believed to result from the inability of *FLNC* to dimerize and cross-link with actin at the C-terminal end of *FLNC*. The absence of *FLNC* protein aggregates in our study and in the series of Ortiz-Genga et al. (12), is again more in line with a haploinsufficiency model.

The highly arrhythmogenic phenotype and the pattern of biventricular subepicardial fibrosis and fatty infiltration seen in 2 siblings from family DNFDC057 is more reminiscent of features previously described specifically in left-dominant arrhythmogenic cardiomyopathy and *PLN* R14del cardiomyopathy (31) rather than classical ARVC. For example, reduced junctional signal for desmoplakin, seen in both the heart and buccal mucosa in siblings from family DNFDC057, is more closely linked with biventricular involvement. Similarly, changes in the distribution of cell-cell junction proteins in the heart and buccal mucosa of these patients are more typical of left-dominant arrhythmogenic cardiomyopathy than classical ARVC. Interestingly, we also observed reduced signal for the membrane-associated guanylate kinase protein SAP97 in both the heart and buccal mucosa in 2 siblings from kindred DNFDC057. Such reduced SAP97 signal has been implicated in abnormal trafficking of ion channel proteins involved in channeling sodium and potassium ions, specifically related to regulating the I_{Na} , and I_{K1} currents, which help maintain normal cardiac ventricular resting membrane action potential (27). This may be relevant to the highly arrhythmogenic phenotype seen in our patients: reduced junctional signals for plakoglobin and Cx43 and translocation of GSK3 β to cell-cell junctions are all features consistently seen in classical ARVC, but were not seen in our patients. Finally, although we have previously shown that buccal mucosa cells exhibit changes similar to those seen in the hearts of ARVC patients (24), studies here are the first to directly compare buccal cells and myocardium from the same patients. These results add further credence to the idea that changes in the heart of complex familial arrhythmia syndromes may also be seen in the buccal mucosa.

STUDY LIMITATIONS. Our study may be limited by the low frequency of *FLNC* truncations, the inability to perform extensive segregation analysis due to small family sizes, and an incomplete availability of DNA samples from biological members of *FLNC* truncation families. Efforts to recruit additional family members, especially reportedly affected

individuals, have not been fruitful to date. In addition, cardiac tissue was only available from 1 family (2 siblings), which hinders our ability to systematically evaluate the effects of different variants on cardiac cellular structure and function. The presence of a variant in another DCM-related gene (*SCN5A*) in combination with the *FLNC* truncation variant in patient TSFDC043 I:1 presents an additional confounding variable. Although all patients are routinely examined for muscle wasting, rigidity, muscle strength, and coordination, invasive skeletal muscle studies that may reveal more subtle pathology, such as electromyography and muscle biopsy, were not performed. Additional phenotypic characterization, such as with contrast-enhanced cardiac magnetic resonance, was also not done in our population. Finally, future studies are needed to elucidate how *FLNC* truncation variants lead to cardiomyocyte dysfunction and cardiac muscle disease.

CONCLUSIONS

Our report provides new evidence that *FLNC* truncation variants are associated with a severe arrhythmogenic DCM phenotype in the absence of overt skeletal muscle disease. *FLNC* should be included in DCM genetic testing panels, particularly when arrhythmias complicate the presenting phenotype. Additionally, patients with *FLNC* truncation variants should be clinically monitored for arrhythmias and considered for implantable cardioverter-defibrillators. Histological and ultrastructural analysis of heart muscle showed no protein aggregates as described in MFM, but instead showed biventricular subepicardial fibrofatty infiltration, Z-disc abnormalities, and redistribution of cell-cell junction proteins. We theorize that haploinsufficiency of *FLNC* (9) may disrupt its normal functions of cross-linking actin filaments, connecting subsarcolemmal sarcomere Z-discs to the cell membrane and integrins, and connecting actin to cell-cell adhesion junctions in intercalated discs, to result in interference with the desmosomal/cell-cell junction pathway and manifest as a phenotypically arrhythmogenic cardiomyopathy.

ACKNOWLEDGMENTS The authors thank the families who contributed to the project by participating in this study, as well as Keona Begay for assistance in editing the *FLNC* map and other figures.

ADDRESS FOR CORRESPONDENCE: Dr. Matthew Taylor, Cardiovascular Institute and Adult Medical Genetics Program, University of Colorado Denver, 12700 East 19th Avenue, Room P15-8022, Aurora, Colorado 80045. E-mail: matthew.taylor@ucdenver.edu.

PERSPECTIVES

COMPETENCY IN MEDICAL KNOWLEDGE: As the number of genes associated with DCM continues to increase, differences in clinical presentations are becoming recognized. Patients with *FLNC* truncation variants should be clinically monitored for arrhythmias and considered for implantable cardioverter-defibrillator devices.

TRANSLATIONAL OUTLOOK: DCM is a common cause of heart failure and life-threatening arrhythmias, and it is frequently caused by gene mutations. The whole spectrum of genetic determinants of DCM is still unknown:

however, recently, a novel disease gene known to cause muscular dystrophy, filamin C, has been reported in human dilated cardiomyopathy and zebrafish models. Here, we report that *FLNC* truncating variants are not rare, are associated with a cardiac-restricted phenotype, are characterized by a high risk of life-threatening ventricular arrhythmias, and are a pathological cellular phenotype affecting the cell-cell adhesion structures, which partially overlaps with ARVC.

REFERENCES

- Haas J, Frese KS, Peil B, et al. Atlas of the clinical genetics of human dilated cardiomyopathy. *Eur Heart J* 2015;36;18:1123-35a.
- Daughenbaugh LA. Cardiomyopathy: an overview. *J Nurse Pract* 2007;3:248-58.
- Hershberger RE, Hedges DJ, Morales A. Dilated cardiomyopathy: the complexity of a diverse genetic architecture. *Nat Rev Cardiol* 2013;10(9):531-47.
- Kley RA, Serdaroglu-Ofazer P, Leber Y, et al. Pathophysiology of protein aggregation and extended phenotyping in filaminopathy. *Brain* 2012;135 pt 9:2642-60.
- Gontier Y, Taivainen A, Fontao L, et al. The Z-disc proteins myotilin and FATZ-1 interact with each other and are connected to the sarcolemma via muscle-specific filamins. *J Cell Sci* 2005;118 pt 16:3739-49.
- Furst DO, Goldfarb LG, Kley RA, Vorgerd M, Olive M, van der Ven PF. Filamin C-related myopathies: pathology and mechanisms. *Acta Neuropathol* 2013;125:33-46.
- Valdes-Mas R, Gutierrez-Fernandez A, Gomez J, et al. Mutations in filamin C cause a new form of familial hypertrophic cardiomyopathy. *Nat Commun* 2014;5:5326.
- Brodehl A, Ferrier RA, Hamilton SJ, et al. Mutations in *FLNC* are associated with familial restrictive cardiomyopathy. *Hum Mutat* 2016;37:269-79.
- Begay RL, Tharp CA, Martin A, et al. *FLNC* gene splice mutations cause dilated cardiomyopathy. *J Am Coll Cardiol Basic Trans Science* 2016;1:344-59.
- Deo RC, Musso G, Tasan M, et al. Prioritizing causal disease genes using unbiased genomic features. *Genome Biol* 2014;15:534.
- Golbus JR, Puckelwartz MJ, Dellefave-Castillo L, et al. Targeted analysis of whole genome sequence data to diagnose genetic cardiomyopathy. *Circ Cardiovasc Genet* 2014;7:751-9.
- Ortiz-Genga MF, Cuenca S, Dal Ferro M, et al. Truncating *flnc* mutations are associated with high-risk dilated and arrhythmogenic cardiomyopathies. *J Am Coll Cardiol* 2016;68:2440-51.
- Spezzacatene A, Sinagra G, Merlo M, et al. Arrhythmogenic phenotype in dilated cardiomyopathy: natural history and predictors of life-threatening arrhythmias. *J Am Heart Assoc* 2015;4:e002149.
- Mestroni L, Maisch B, McKenna WJ, et al., from the Collaborative Research Group of the European Human and Capital Mobility Project on Familial Dilated Cardiomyopathy. Guidelines for the study of familial dilated cardiomyopathies. *Eur Heart J* 1999;20:93-102.
- Rowland TJ, Graw SL, Sweet ME, Gigli M, Taylor MR, Mestroni L. Obscurin variants in patients with left ventricular noncompaction. *J Am Coll Cardiol* 2016;68:2237-8.
- Wu TD, Nacu S. Fast and SNP-tolerant detection of complex variants and splicing in short reads. *Bioinformatics* 2010;26(7):873-81.
- Wang K, Li M, Hakonarson H. ANNOVAR: functional annotation of genetic variants from high-throughput sequencing data. *Nucleic Acids Res* 2010;38:e164.
- Liu X, Jian X, Boerwinkle E. dbNSFP: a lightweight database of human nonsynonymous SNPs and their functional predictions. *Hum Mutat* 2011;32:894-9.
- Campbell N, Sinagra G, Jones KL, et al. Whole exome sequencing identifies a troponin T mutation hot spot in familial dilated cardiomyopathy. *PLoS One* 2013;8:e78104.
- Abecasis GR, Auton A, Brooks LD, et al. An integrated map of genetic variation from 1,092 human genomes. *Nature* 2012;491(7422):56-65.
- NHLBI Go Exome Sequencing Project (ESP). Available at: <http://evs.gs.washington.edu/EVS/>. Accessed October 17, 2016.
- Lek M, Karczewski KJ, Minikel EV, et al. Exome Aggregation, C. Analysis of protein-coding genetic variation in 60,706 humans. *Nature* 2016;536(7616):285-91.
- Landrum MJ, Lee JM, Benson M, et al. ClinVar: public archive of interpretations of clinically relevant variants. *Nucleic Acids Res* 2016;44:D862-8.
- Asimaki A, Protonotarios A, James CA, et al. Characterizing the molecular pathology of arrhythmogenic cardiomyopathy in patient buccal mucosa cells. *Circ Arrhythm Electrophysiol* 2016;9:e003688.
- Marcus FI, McKenna WJ, Sherrill D, et al. Diagnosis of arrhythmogenic right ventricular cardiomyopathy/dysplasia: proposed modification of the Task Force Criteria. *Eur Heart J* 2010;31:806-14.
- Asimaki A, Tandri H, Huang H, et al. A new diagnostic test for arrhythmogenic right ventricular cardiomyopathy. *N Engl J Med* 2009;360:1075-84.
- Asimaki A, Kapoor S, Plovie E, et al. Identification of a new modulator of the intercalated disc in a zebrafish model of arrhythmogenic cardiomyopathy. *Sci Transl Med* 2014;6(240):240ra274.
- Chelko SP, Asimaki A, Andersen P, et al. Central role for GSK3beta in the pathogenesis of arrhythmogenic cardiomyopathy. *JCI Insight* 2016;1:e85923.
- Zhou AX, Hartwig JH, Akyurek LM. Filamins in cell signaling, transcription and organ development. *Trends in cell biology* 2010;20:113-23.
- Kley RA, Hellenbroich Y, van der Ven PF, et al. Clinical and morphological phenotype of the filamin myopathy: a study of 31 German patients. *Brain* 2007;130 pt 12:3250-64.
- van der Zwaag PA, van Rijsingen IA, Asimaki A, et al. Phospholamban R14del mutation in patients diagnosed with dilated cardiomyopathy or arrhythmogenic right ventricular cardiomyopathy: evidence supporting the concept of arrhythmogenic cardiomyopathy. *Eur J Heart Fail* 2012;14:1199-207.

KEY WORDS arrhythmias, arrhythmogenic dilated cardiomyopathy, cardiovascular genetics, Filamin C, familial dilated cardiomyopathy, heart failure

APPENDIX For expanded Methods and Results sections, as well as supplemental figures and tables, please see the online version of this paper.